Effect of the interaction of components in a nickel-molybdenum catalyst on its activity in decomposition of methane to hydrogen

N.M. Makayeva*, G.E. Yergazieva, M.M. Anisova, J. Shaimerden, K. Dossumov

Institute of Combustion Problems, Almaty, Kazakhstan
*E-mail: *nursaya.1996.mk@mail.ru*

This work is devoted to the study of the activity of monometallic (Fe/Al_2O_3) and bimetallic ($Fe\text{-}Mo/Al_2O_3$) catalysts supported to carrier γ- Al_2O_3 It has been discovered that the bimetallic catalyst is more active than the monometallic catalyst in the methane decomposition reaction. The results of the influence of molybdenum oxide on the activity of Fe/Al_2O_3 catalyst in the methane decomposition reaction in the temperature range 500-850°C have been obtained. It has been determined that the addition of molybdenum oxide in the amount of 5 wt. % of the iron catalyst composition leads to an increase in the catalytic activity of the sample in the reaction of methanedecomposition to hydrogen at relatively low temperatures. Compared to Fe/Al_2O_3 on the $FeMo/Al_2O_3$ catalyst at a reaction temperature of 750°C, methane conversionincreases from 8% to 98%, hydrogen yield from 5% to 57%.

The increased field of activity $Fe\text{-}Mo/Al_2O_3$catalyst in the decomposition of methane to hydrogen compared to Fe/Al_2O_3 catalysts is due to an increase in the dispersity of the active phases of the catalyst, as well as the formation of an easily reduced $Fe_2(MoO_4)_3$ phase, according to XRD, TPR-H_2, and BET methods.

Keywords: iron oxide; molybdenum oxide; methane; decomposition; hydrogen.

Никель-молибден катализаторындағы компоненттердің өзара әрекеттесуінің оның метанның сутекке дейін ыдырауында белсенділігіне әсері

Н.М. Макаева*, Г.Е. Ергазиева, М.М. Анисова, Ж. Шаймерден, К. Досумов

Жаңу мәселелері институты, Алматы қ., Қазақстан
*E-mail: *nursaya.1996.mk@mail.ru*

Бұл жұмыс γ-Al_2O_3 тасымалдағышына отырғызылған монометалды (Fe/Al_2O_3) және биметалды ($Fe\text{-}Mo/Al_2O_3$) катализаторлардың белсенділігін зерттеуге арналған. Метанның ыдырау реакциясында монометалды катализаторға қарағанда биметалды катализатордың белсендірек екені анықталды. Метанның ыдырау реакциясында 500-850°C температура диапазонында молибден оксидінің Fe/Al_2O_3 катализатор белсенділігіне әсер ету нәтижелері алынды. Темір катализаторының құрамына 5 мас.% мөлшерінде молибден оксидінің қосылуы салыстырмалы төменгі температурада метанның сутекке дейінгі ыдырау реакциясында үлгінің каталитикалық белсенділігін арттыратындығы анықталды. 750°C реакция температурасында Fe/Al_2O_3-пен салыстырғанда $Fe\text{-}Mo/Al_2O_3$ катализаторында метанның конверсиясы 8%-дан 98%-ға дейін, сутектің шығымы 5%-дан 57%-ға дейін артатыны байқалған. РҚТ, Н2-ТБТ және БЭТ әдістері метанның сутекке ыдырау процесі кезінде Fe/Al_2O_3 катализаторымен салыстырғанда $Fe\text{-}Mo/Al_2O_3$ белсенділігінің артуы, белсенді фазалардың дисперсиясының жоғарылауымен, сондай-ақ жеңіл тотықсызданатын $Fe_2(MoO_4)_3$ фазасының түзілуімен байланысты екенін көрсетті.

Түйін сөздер: темір оксиді; молибден оксиді; метан; ыдырау; сутек.

Влияние взаимодействия компонентов в никель-молибденовом катализаторе на его активность в разложении метана до водорода

Н.М. Макаева*, Г.Е. Ергазиева, М.М. Анисова, Ж. Шаймерден, К. Досумов

Институт проблем горения, г. Алматы, Казахстан
*E-mail: nursaya.1996.mk@mail.ru

Данная работа посвящена исследованию активности монометаллических (Fe/Al_2O_3) и биметаллических ($Fe\text{-}Mo/Al_2O_3$) катализаторов, нанесенных на носитель γ-Al_2O_3. Установлено, что в реакции разложения метана биметаллический катализатор более активен, чем монометаллический. Получены результаты влияния оксида молибдена на активность катализатора Fe/Al_2O_3 в реакции разложения метана в температурном диапазоне 500-850°C. Установлено, что добавление оксида молибдена в количестве 5 мас. % в состав железного катализатора приводит к повышению каталитической активности образца в реакции разложения метана в водород при относительно низких температурах. По сравнению с Fe/Al_2O_3 на катализаторе $FeMo/Al_2O_3$ при температуре реакции 750 °C, конверсия метана увеличивается от 8% до 98%, выход водорода от 5% до 57%. Согласно результатам РФА, ТПВ-H_2 и БЭТ повышение активности $Fe\text{-}Mo/Al_2O_3$ при разложении метана в водород по сравнению с катализаторами Fe/Al_2O_3 связано с увеличением дисперсности активных фаз катализатора, а также формированием легко восстанавливаемой фазы $Fe_2(MoO_4)_3$.

Ключевые слова: оксид железа; оксид молибдена; метан; разложение; водород.

(2022) Chem Bull Kaz Nat Univ 3:12-19

CHEMICAL BULLETIN
of Kazakh National University
http://bulletin.chemistry.kz/

UDC 54.54 https://doi.org/10.15328/cb1281

Effect of the interaction of components in a nickel-molybdenum catalyst on its activity in decomposition of methane to hydrogen

N.M. Makayeva*, G.E. Yergazieva, M.M. Anisova, J. Shaimerden, K. Dossumov

Institute of Combustion Problems, Bogenbay Batyr str. 172, 050000 Almaty, Kazakhstan
*E-mail: *nursaya.1996.mk@mail.ru*

1. Introduction

The direct transformation of methane into value-added chemicals is one of the most important topics in gas chemistry. Methane can synthesize the entire range of products made from oil. The cost of substances like synthesis gas, hydrogen and ethylene is many times higher than the original CH_4. Methane is the best source of hydrogen since it has the highest C-H ratio and the largest reserves.

From methane, hydrogen can be obtained from the following reactions using catalysts: partial oxidation of methane [1], carbon dioxide conversion of methane [2], steam conversion of methane [3], catalytic decomposition of CH_4 [4]. Catalytic decomposition of methane (CDM), the most cost-effective method for producingH_2. The catalytic decomposition is methane positive by the reaction shown in Equation 1.

$$CH_4 \rightarrow 2H_2 + C \quad \Delta H = 74.9 \text{ kJ mol}^{-1} \qquad (1)$$

The main advantage of CDM is the almost complete absence of carbon monoxide emissions. In addition, CDM to hydrogen can be utilized directly as a fuel cell in internal combustion engines without the need for extra cleaning [5]. In addition, the nanocarbon produced, which has many technological applications, reduces the cost of the process.

Various catalysts based on nickel, carbon, precious metals, iron, etc. are used to decompose methane.

Previously, the authors studied monometallic and bimetallic nickel-containing catalysts [6]. The results obtained showed that the modification of Ni/Al_2O_3 with cobalt oxide leads to an increase in the activity of the catalyst in the reaction of methane decomposition to hydrogen and nano-carbon due to the formation of the NiCo alloy. On the $Ni\text{-}Co/\gamma\text{-}Al_2O_3$ catalyst, the highest methane conversion of 86% was observed at a reaction temperature of 600°C, with a hydrogen yield of 51%. However, the catalytic activity of the bimetallic $Ni\text{-}Co/\gamma\text{-}Al_2O_3$ decreased after 60 min. The results obtained indicate that nickel-based catalysts have a high activity in CDM, however, they are sensitive to the operating temperature and quickly deactivate at high temperatures [7,8]. Although adding precious metals to nickel-based catalysts can increase activity and stability, it is rather costly and has no commercial potential. Carbon catalysts convert methane at a lower rate than metal catalysts [9].

To make the CDM to H_2truly environmentally sound and economical, the use of a very cheap catalyst is a promising approach [10]. A highly efficient and environmentally friendly iron catalyst is an effective alternative to solving the problem at present [11]. In addition, iron is a good candidate for use as a CDM catalyst, as it also has unfilled 3d orbitals [11,12].

To increase the activity of iron composites, oxides of transition elements such as nickel, copper, manganese, molybdenum are added. In some studies, yield of hydrogenis reported to increase when a certain amount of molybdenum is added to Fe [13], Co [14] and Ni [15]. The physicochemical characteristics of Fe–Mo catalysts were studied in this work [16]. Until now, the role of molybdenum in the bimetallic catalyst is unclear. There are conflicting data in the literature. It is also not clear why the catalytic nature of the bimetallic Fe–Mo catalyst is better than that of the monometallic (Fe and Mo) catalyst [1-6,17].

In this work, a comparative study of the activity of monometallic (Fe/Al_2O_3) and bimetallic ($Fe\text{-}Mo/Al_2O_3$) catalysts was carried out, which is a novelty of this work.

The aim of this work is to study the activity of monometallic (Fe/Al_2O_3) and bimetallic ($Fe\text{-}Mo/Al_2O_3$) catalysts, to determine the effect of the interaction of components in a nickel-molybdenum catalyst on its activity in hydrogen production by methane decomposition.

2. Experiment

Catalysts xFe/Al_2O_3 and $xFe\text{-}yMo/Al_2O_3$(x and y are the content of metal oxides in the catalyst, wt. %) were obtained by impregnating the carrier (γ-Al_2O_3) with aqueous metal salt solutions $Fe(NO_3)_3 \cdot 9H_2O$ (technical standard 4111-74, Sigma Aldrich, reagent grade 98%) and mixtures $Fe(NO_3)_3 \cdot 9H_2O$ (technical standard 4111-74, Sigma Aldrich, reagent grade 98%) and $(NH_4)_6Mo_7O_{24} \cdot 4H_2O$ (technical standard 3765-78, Sigma Aldrich, reagent grade 99%), respectively [17,18]. Heat treatment of synthesized catalysts was carried out at temperatures of 300°C for 2 hours and at 500°C for 3 hours. The oxide content of Fe in the monometallic catalyst was 15 wt.%, in bimetal 15 wt.% Fe and 5 wt.% Mo.

Studies of the activity of synthesized catalysts was carried out at a laboratory with a continuous flow facility (Figure 1). The reactor is made of quartz glass, length 22-25 cm, internal diameter – 10 mm. The reactor is vertically installed in the furnace, and the incoming flow of the source gas mixture is fed into the reactor through a pipe with a diameter of 0.6 mm from the top and exits through an opening in the lower part of the reactor. Further online line is submitted for analysis in chromatograph "Chromos GC – 1000". Catalytic activity of catalysts has been studied with a volumetric reaction rate of 4980 h^{-1} and a volume ratio of the original reagents CH_4:N_2=1:15, within a temperature range of 500-850ºC.The following gases were used for the experiments:CH_4 (NTC «Kriogen», Russia, purity 99.9%), N_2 (NTC «Kriogen», Russia, purity 99.9%), H_2 (NTC «Kriogen», Russia, purity 99.9%). All reagents were used without additional purification.

The physicochemical characteristics of the catalysts were studied by X-ray phase analysis (XRD), Brunauer-Emmett-Taylor (BET), temperature-programmed hydrogen reduction (H_2-TPR), and Raman spectroscopy. The research was carried out at Al-Faraby KazNU"National Nanotechnology Laboratory of open type" and in the laboratory of catalytic processes of the Institute of Combustion Problems. H_2 temperature-programmed reduction (H_2-TPR) was carried out in on USGA-101 installation with thermal conductivity detector. Analysis of the gas mixture was carried out using a thermal conductivity detector. X-ray analysis of the obtained samples was carried out on the X-ray diffractometer "DRON-3M". To determine the total specific surface size by thermal desorption of the gas-adsorbate method was performed by the BET method in accordance with State All-Union standard 23401-90.

3. Results and Discussion

Table 1 shows that the monometallic $Fe/\text{-}Al_2O_3$ catalyst has a specific surface of 122.73 m^2/g and that adding molybdenum oxide increases the specific surface to 134.82 m^2/g, which indicates an increase in the dispersity of the catalyst.

Table 1 – Texture characteristics of catalysts

Catalysts applied to γ-Al_2O_3	Specific surface, m^2/g
$Fe/\gamma\text{-}Al_2O_3$	122.73
$Fe\text{-}Mo/\gamma\text{-}Al_2O_3$	134.82

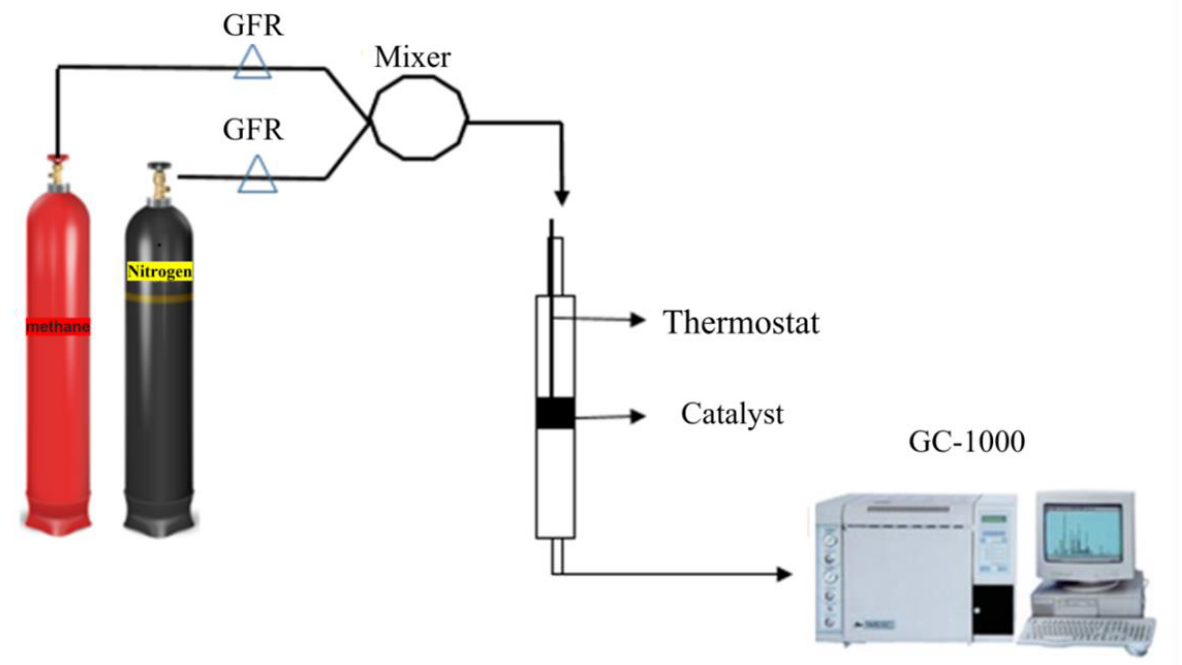

Figure 1 – Laboratory catalytic unit schematic

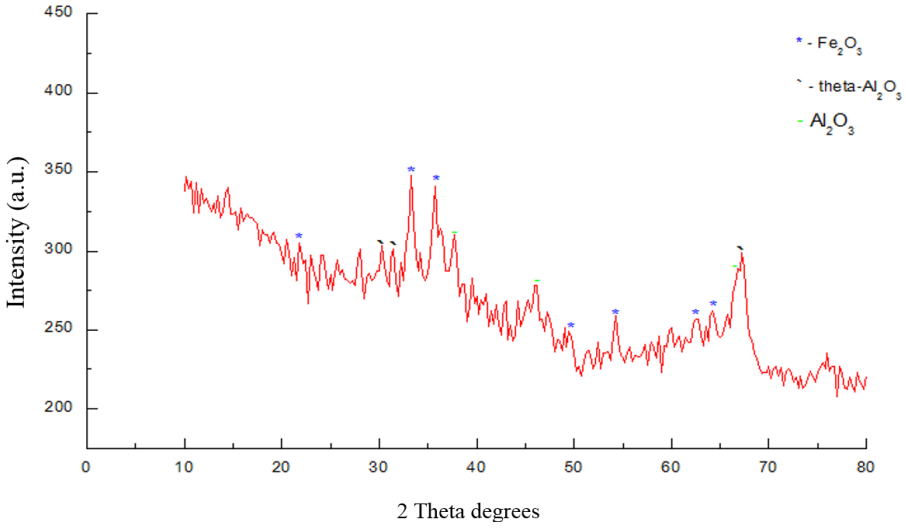

Figure 2 – X-ray Fe/γ-Al_2O_3

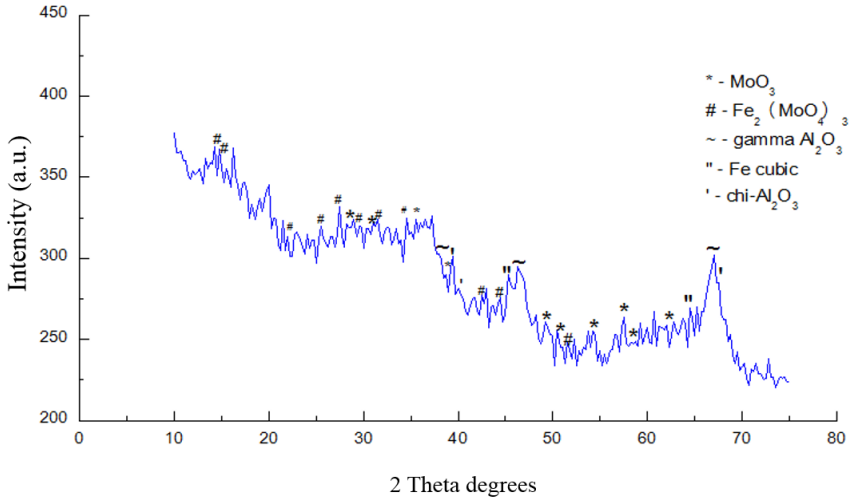

Figure 3 – X-rayFe-Mo/γ-Al_2O_3

The results of the Fe/γ-Al_2O_3, Fe-Mo/γ-Al_2O_3 catalyst phase-compositions are shown in Figures 2 and 3. It can be seen that iron is present as oxide Fe_2O_3 in the catalyst Fe/γ-Al_2O_3. Modification of Fe/γ-Al_2O_3 by molybdenum oxide results in a change in catalyst phase composition, iron is present in the form of Fecubic, molybdenum in the form of MoO_3 oxide, and a $Fe_2(MoO_4)_3$ compound is formed.

Oxidative-reducing characteristics of catalysts have been studied by TPR-H_2. The results are presented in Figure 4.

On the TPR profile of Fe/Al_2O_3 there is an intense peak with maximum at T^1_{max}=434°C, (A=342 μmol/gKt), also low-intensity peaks above 660°C. According to the literature [8], Fe_2O_3 is reduced to Fe^0 successively at temperatures of ~350, 430, and 600°C. However, the reduction temperature of Fe_2O_3 can be shifted both to the low-temperature and high-temperature regions, depending on the nature of the substrate, modifiers,

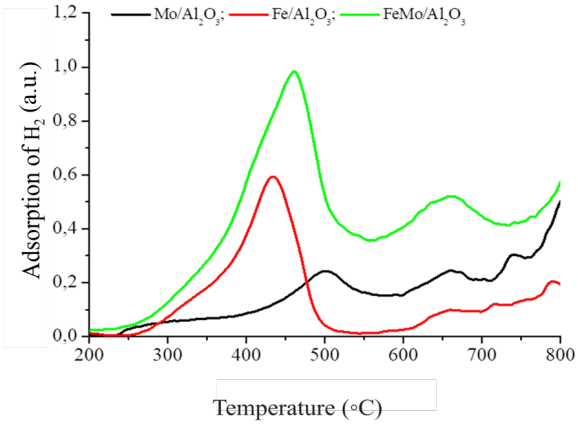

Figure 4 – TPR profiles

and other factors. The peak at T^1_{max}=434°C on the Fe/Al_2O_3 TPR profile can be associated with Fe_3O_4 → FeO reduction, Fe_2O_3 → Fe_3O_4 reduction is not observed, possibly due to the overlap of the Fe_3O_4 peak.

Peaks in the region of 650-720°C can be attributed to FeO reduction. The presence of several peaks may indicate the interaction of the metal-carrier, characterized by different strengths.

On the TPR profile of 5wt.% $Mo/\gamma\text{-}Al_2O_3$ catalyst have three peaks with maxima at T^1_{max}=502°C, (Hydrogen quantity A=55 µmol/gKt), T^2_{max}=660°C, (A=19 µmol/gKt) and T^3_{max}=741°C, (A=7 µmol/gKt).

The conversion of Mo^{6+} to Mo^{4+} in distributed Mo structures is generally linked with a low temperature peak around T^1_{max}=502°C [9]. $MoO_3$is responsible for the peak observed at T^2_{max}=660°C [10]. There is no big peak on the TPR profile at T^3_{max}=741°C, which is linked to further reduction of partially recovered Mo particles from the first and second peaks, as well as partial reduction of strongly interacting tetrahedral coordinated Mo particles with Al_2O_3 [11].

The influence of molybdenum on TPR profile of $Fe/\gamma\text{-}Al_2O_3$ is noticeable, the reduction temperature of Fe_2O_3 is shifted to a high temperature region from 434→461°C, the amount of hydrogen spent on reduction from 342 to 534 µmol/gKt is increased. An increase in the amount of hydrogen consumed and a shift in the reduction temperature can be associated with the formation of the $Fe_2(MoO_4)_3$ phase, since according to [19], this phase is reduced in the range of 400-500°C. According to the literature [12], the formation of the $Fe_2(MoO_4)_3$ phase leads to an increase in the reducibility of iron oxide. Modification of $Fe/\gamma\text{-}Al_2O_3$ with molybdenum oxide leads to an increase in the intensity of the peak with T^2_{max}=660°C, which refers to the reduction of FeO to metallic iron. According to [20] Fe^0 is the center for activating the decomposition of methane.

The catalytic properties of synthesized catalysts in methane decomposition have been investigated in a temperature range of 500-850ºC, the results are presented in Figure 5.

The decomposition of methane on the Fe/Al_2O_3 monometallic catalyst increases from 9% to 99% when the temperature of the methane decomposition process is raised from 500 to 850°C, as shown in the figure.

Figure 5a shows the dependence of methane conversion on the reaction temperature on the Fe/Al_2O_3 catalyst. As can be seen from Figure 5a, the Fe/Al_2O_3 monometallic catalyst has a low conversion in the range of 500–750°C, and the catalyst activity increases with an increase in the reaction temperature. At 850°C, the conversion of methane reaches 99%, the main reaction product in the gas phase is hydrogen (Figure 5b).

The addition of molybdenum oxide to the Fe/Al_2O_3 catalyst increases the catalyst's activity at a lower reaction temperature of 750°C, resulting in a 99% conversion of methane (Figure 5c), which is higher by ~20% compared to the activity of the known catalyst $FeMo(5.1)/Al_2O_3$ [21]. A bimetallic catalyst yields 57%

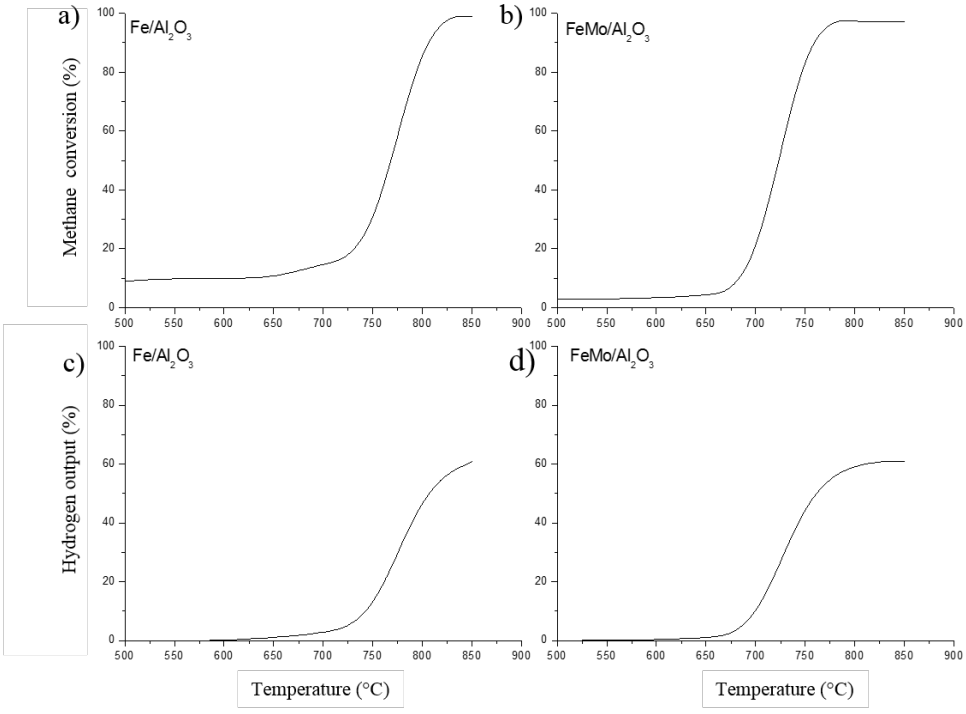

Figure 5 – Influence of reaction temperature on catalyst performance:
methane conversion over Fe/Al_2O_3 (a), methane conversion over $FeMo/Al_2O_3$ (b), yield of hydrogen over Fe/Al_2O_3 (c), yield of hydrogen over $FeMo/Al_2O_3$ (d)

hydrogen at 750°C, while a monometallic catalyst yields just 5% hydrogen (Figure 5d). The increase in the activity of the bimetallic catalyst compared to the monometallic one is possibly associated with an increase in the dispersity of the catalyst, the formation of an easily reduced $Fe_2(MoO_4)_3$ phase, and an increase in the amount of Fe^0, which is the active site of methane activation [22].

Only hydrogen is generated in gas products; no ethylene, ethane, or carbon oxides were found, which indicates the selective course of the reaction of decomposition of methane to hydrogen and carbon [23]. The principal product of the process is hydrogen, as evidenced by a comparison of methane conversion outcomes and hydrogen production.

Catalysts Fe/Al_2O_3 and $FeMo/Al_2O_3$ were tested at a reaction temperature of 750°C in the decomposition of methane for 300 min (Figure 6).

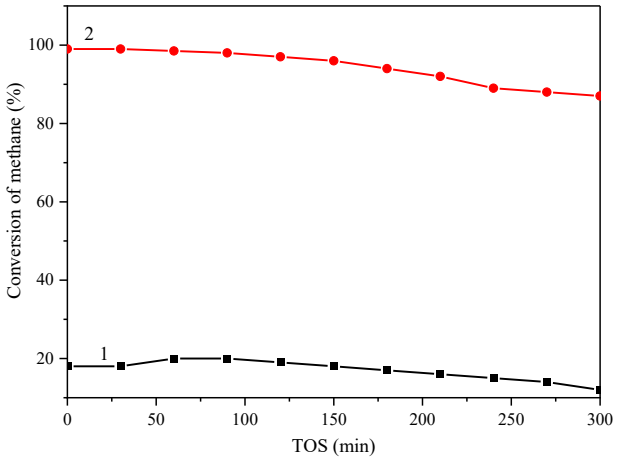

Figure 6 – Stability performance in terms of methane conversion over catalysts: 1 – Fe/Al_2O_3; 2 – $FeMo/Al_2O_3$.

The conversion profiles showed that Fe/Al_2O_3 had a low initial conversion of 19%, which decreased starting at 100 minutes and reached 8% at 300 min. The $FeMo/Al_2O_3$ bimetallic catalyst had an initial conversion of 99%, which gradually decreased and reached 87% at 300 min. If compared with bimetallic catalysts known in the literature 50% Ni-10%Fe/Al_2O_3, $FeMo(5.1)/Al_2O_3$, then the activity and stability of the $FeMo/Al_2O_3$ catalyst are much higher [21,24].

The $FeMo/Al_2O_3$ catalyst after testing at 750°C in the reaction of methane decomposition for 300 min was examined by Raman spectroscopy, the result is shown in Figure 7.

Raman spectra show the presence of D, G and 2D bands. It is known that the G band at 1578 cm^{-1} refers to the vibration of graphite in the C-C plane. The band at 1359 cm^{-1} is called the D band obtained from imperfect graphite. The 2D band (~2716 cm^{-1}) is characteristic of structures with several layers of graphene and graphite. Similar spectra are found in the literature for multilayer graphene and graphite. It is known

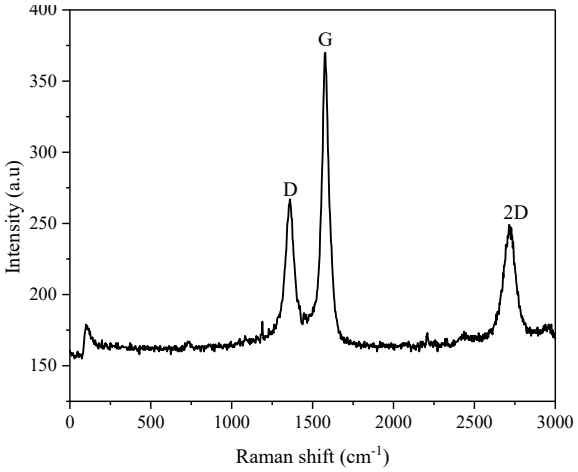

Figure 7 – Raman spectra of the carbon layer on the surface $FeMo/Al_2O_3$ catalyst after the methane decomposition

that the ratio between the intensities of the 2D peak (I2D) and the G peak (IG) gives an estimate of the number of layers. The I2D/IG value of deposited carbon on $FeMo/Al_2O_3$ is 0.66. According to [25], the ratio I2D/IG=0.0.66 indicates 3 layers of graphene.

4. Conclusion

The effect of molybdenum oxide on the activity of the Fe/Al_2O_3 catalyst in the decomposition of methane in the temperature range 500-850°C was studied. It has been determined that the addition of molybdenum oxide in an amount of 5 wt.% to the composition of the iron catalyst leads to an increase in the catalytic activity of the sample in the decomposition of methane to hydrogen at relatively low temperatures. Compared to Fe/Al_2O_3 on the FeMo/ Al_2O_3 catalyst at a reaction temperature of 750°C, the methane conversion increases from 8 to 98%, the hydrogen yield from 5 to 57%. According to Raman spectroscopy, a three-layer graphene-like carbon is formed on the surface of the FeMo/ Al_2O_3 catalyst.

According to the results of XRD, TPR-H_2, and BET, the modification of a monometallic iron composite with molybdenum oxide leads to an increase in the dispersity of the sample and the formation of an easily reduced $Fe_2(MoO_4)_3$ phase. Due to the formation of an easily reduced $Fe_2(MoO_4)_3$ phase, the concentrations of metal particles increase, which are the centers for methane activation.

Acknowledgments

Research financed by the Science Committee of the Ministry of Education and Science of the Republic of Kazakhstan (grant AP08855564).

References (GOST)

1 Zhang J., Li X., Chen H., Qi M., Zhang G., Hu H., Ma X. (2017) Hydrogen production by catalytic methane decomposition: Carbon materials as catalysts or catalyst supports // International Journal of Hydrogen Energy. – 2017. – Vol.42. – P.19755-19775.

2 Usman M., Daud W.M.A., Abbas H.F. Dry reforming of methane: Influence of process parameters—A review // Renewable and Sustainable Energy Reviews. – 2015. – Vol.45. – P.710-744.

3 Osman A.I. Catalytic hydrogen production from methane partial oxidation: mechanism and kinetic study mini-review // Chemical Engineering & Technology. – 2020. – Vol.43. – P.641-648.

4 Chaubey R., Sahu S., James O.O., Maity S.A review on development of industrial processes and emerging techniques for production of hydrogen from renewable and sustainable sources // Renewable and Sustainable Energy Reviews. – 2013. – Vol.23. – P.443-462.

5 Stephens-Romero S., Carreras-Sospedra M., Brouwer J., Dabdub D., Samuelsen S. Determining air quality and greenhouse gas impacts of hydrogen infrastructure and fuel cell vehicles // Environmental Science & Technology. – 2009. – Vol.43. – P.9022-9029.

6 Yergazieva G., Makayeva N., Shaimerden Zh., Soloviev S., Telbayeva M., Akkazin E., Ahmetova F. Catalytic decomposition of methane to hydrogen over Al2O3 supported mono-and bimetallic catalysts // Bulletin of Chemical Reaction Engineering & Catalysis. – 2022. – Vol.17. – P.1-12.

7 Ermakova M.A., Ermakov D.Y., KuvshinovG.G. Effective catalysts for direct cracking of methane to produce hydrogen and filamentous carbon: Part I. Nickel catalysts // Applied Catalysis A: General – 2000. – Vol.201. – P.61-70.

8 Zhang J., Jin L., Li Y., Hu H. Ni doped carbons for hydrogen production by catalytic methane decomposition // International Journal of Hydrogen Energy. – 2013. – Vol.38. – P.3937-3947.

9 Serrano D.P., Botas J.A., Fierro J.L.G., Guil-López R., Pizarro P., Gómez G. Hydrogen production by methane decomposition: origin of the catalytic activity of carbon materials // Fuel. – 2010. – Vol.89. – P.1241-1248.

10 Bai Z., Chen H., Li B., Li W. Methane decomposition over Ni loaded activated carbon for hydrogen production and the formation of filamentous carbon // International Journal of Hydrogen Energy. – 2007. – Vol.32. – P.32-37.

11 Jin L., Si H., Zhang J., Lin P., Hu Z., Qiu B. et al. Preparation of activated carbon supported Fe–Al2O3catalyst and its application for hydrogen production by catalytic methane decomposition // International Journal of Hydrogen Energy. – 2013. – Vol.38. – P.1-8.

12 Awadallah A.E., Aboul-Enein A.A., Mahmoud A.H., Abd El Rehim S.S., El-Ziaty A.K., Aboul-GheitA.K. Zr x Mg 1-x O supported cobalt catalysts for methane decomposition into CO x -free hydrogen and carbon nanotubes// International Journal of Green Energy. – 2018. – Vol.15. – P.568-576.

13 Christen H.M., Puretzky A.A., Cui H., Belay K., Fleming P.H., Geohegan D.B., Lowndes D.H. Nano Lett. Rapid growth of long, vertically aligned carbon nanotubes through efficient catalyst optimization using metal film gradients // Chemistry. – 2004. – Vol.10. – P.1939-1942.

14 Hu M., Murakami Y., Ogura M., Maruyama S., Okubo T. Morphology and chemical state of Co–Mo catalysts for growth of single-walled carbon nanotubes vertically aligned on quartz substrates // Chemistry. – 2004. – Vol.225. – P.230-239.

15 Li Y., Zhang X.B., Tao X.Y., Xu J.M., Huang W.Z., Luo J.H. et al. Highly mesoporous carbon foams synthesized by a facile, cost-effective and template-free Pechini method for advanced lithium–sulfur batteries // Journal of Materials Chemistry. –2005. – Vol.43. – P.295-301.

16 Saito T., Xu W.-C., Ohshima S., Ago H., Yumura M., Iijima S. Diameter-dependent hydrophobicity in carbon nanotubes // The Journal of Chemical Physics. – 2016. – Vol.145. – P.5849-5853.

17 Huilin Y., Qiangqiang X., Shuliang L., Jiajia W., Yujun W., Guangsheng L. Effect of pore structure on Ni/Al_2O_3 microsphere catalysts for enhanced CO_2 methanation // Fuel. – 2022. – Vol.315. – P.123262.

18 Dossumov K., Yergaziyeva G., Ermagambet B., Myltykbaeva L., Telbaeva M. Morphology and catalytic properties of cobalt-containing catalysts synthesized by different means // Russian Journal of Physical Chemistry. – 2020. – Vol.94. – P.880-882.

19 Shouchun M., Yang Y., Jiaqi L., Yuqing M., Yufeng Z., Jie W., Li L., Tongjie Y., Qingfeng Y. Z-scheme Fe2(MoO4)3/Ag/Ag3PO4 heterojunction with enhanced degradation rate by in-situ generated H2O2: Turning waste (H2O2) into wealth (•OH) // Journal of Colloid and Interface Science. – 2022. – Vol.606. – P.1800-1810

20 Jing X., Tian W., Linga R., Da B., Gerard M., Jean-Marie B., Lu Zh. Methane decomposition to produce COx-free hydrogen and nano-carbon over metal catalysts: A review // Hydrogen Energy Publications. – 2020. – Vol.45. – P.7981-8001.

21 Torres D., Pinilla J.L., Lazaro M.J., Moliner R., Suelves I. Hydrogen and multiwall carbon nanotubes production by catalytic decomposition of methane: Thermogravimetric analysis and scaling-up of FeMo catalysts // Hydrogen Energy Publications. – 2014. – Vol.39. –P.3698-3709.

22 Jing X., Da B., Jean M., Lu Zh. Methane decomposition to produce hydrogen and carbon nanomaterials over costless, iron-containing catalysts // Journal of Cleaner Production. – 2021. – Vol.320. – P.879-884.

23 Henao W., Cazaña F., Tarifa P., Romeo E., Latorre N. et al. Selective synthesis of carbon nanotubes by catalytic decomposition of methane using Co-Cu/Cellulose derived carbon catalysts: A comprehensive kinetic study // Chemical Engineering Journal. – 2020. – Vol.20. – P.103-126.

24 Bayat N., Meshkani F., Rezaei M. Thermocatalytic decomposition of methane to COx-free hydrogen and carbon over Ni–Fe–Cu/Al_2O_3 catalysts // International Journal of Hydrogen Energy. – 2016. – Vol.30. – P.13039-13049.

25 Osipov A., Sidorchik I., Shlypin D., Borisov V., Leontieva N., Lacrenov A. Thermocatalytic decomposition of methane on carbon materials and its use in hydrogen energy technologies // Catalysis in Industry. – 2021. – Vol.13. – P.244-251.

References

1 Zhang J, Li X, Chen H, Qi M, Zhang G, Hu H, Ma X (2017) Int J Hydrogen Energ 42:19755-19775. *https://doi.org/10.1016/j.ijhydene.2017.06.197*

2 Usman M, Daud MA, Abbas HF (2015) Renew Sust Energ Rev 45:710-744. *https://doi.org/10.1016/j.rser.2015.02.026*

3 Osman AI (2020) Chem Eng Technol 43:641-648. *https://doi.org/10.1002/ceat.201900339*

4 Chaubey R, Sahu S, James OO, Maity S (2013) Renew Sust Energ Rev 23:443-462. *https://doi.org/10.1016/j.rser.2013.02.019*

5 Stephens-Romero S, Carreras-Sospedra M, Brouwer J, Dabdub D, Samuelsen S (2009) Environ Sci Technol 43:9022-9029. *https://doi.org/10.1021/es901515*

6 Yergazieva G, Makayeva N, Shaimerden Zh, Soloviev S, elbayeva M, Akkazin E, Ahmetova F (2022) Bulletin of Chemical Reaction Engineering & Catalysis 17:1-12. *https://doi.org/10.9767/bcrec.17.1.12174.1-12*

7 Ermakova MA, Ermakov DY, Kuvshinov GG (2000) Applied Catalysis A 201:61-70. *https://doi.org/10.1016/S0926-860X(00)00433-6*

8 Zhang J, Jin L, Li Y, Hu H (2013) International Journal of Hydrogen Energy 38:3937-3947. *https://doi.org/10.1016/j.ijhydene.2013.01.105*

9 Serrano DP, Botas JA, Fierro JLG, Guil-López R, Pizarro P, Gómez G (2010) Origin of the catalytic activity of carbon materials 89:1241-1248. *https://doi.org/10.1016/j.ijhydene.2015.01.056*

10 Bai Z, Chen H, Li B, Li W (2007) Int J Hydrogen Energ 32:32-37. *https://doi.org/10.1016/j.ijhydene.2006.06.030*

11 Jin L, Si H, Zhang J, Lin P, Hu Z, Qiu B (2013) Int J Hydrogen Energ 38:1-8. *https://doi.org/10.1016/j.ijhydene.2013.06.023*

12 Awadallah AE, Aboul-Enein AA, Mahmoud AH, Abd El Rehim SS, El-Ziaty AK, Aboul-Gheit AK (2018) Int J Green Energy 15:568-576. *https://doi.org/10.1016/j.ijhydene.2016.07.081*

13 Christen HM, Puretzky AA, Cui H, Belay K, Fleming PH, Geohegan DB (2004) Nano Lett 10:1939-1942. *https://doi.org/10.1021/nl048856f*

14 Hu M, Murakami Y, Ogura M, Maruyama S, Okubo T, (2004) J Catal 225:230-239. *https://doi.org/10.1016/j.jcat.2004.04.013*

15 Li Y, Zhang XB, Tao XY, Xu JM, Huang WZ, Luo JH, Luo ZQ, Li T, Liu F, Bao Y, Geise HJ (2005) Carbon 43:295-301. *https://doi.org/10.4028/www.scientific.net/SSP.121-123.167*

16 Saito TW, Xu C, Ohshima S, Ago H, Yumura M, Iijima S (2006) Phys Chem B 12:5849-5853. *https://doi.org/10.1063/1.4960609*

17 Huilin Y, Qiangqiang X, Shuliang L, Jiajia W, Yujun W, Guangsheng L (2022) Fuel 315:123262. *https://doi.org/10.1016/j.fuel.2022.123262*

18 Dossumov K, Yergaziyeva G, Ermagambet B, Myltykbaeva L, Telbaeva M (2020) Russ J Phys Ch 94:880-882. *https://doi.org/10.1134/S0036024420040020*

19 Shouchun M, Yang Y, Jiaqi L, Yuqing M, Yufeng Z, Jie W, Li L, Tongjie Y, Qingfeng Y (2022) Journal of Colloid and Interface Science 606:1800-1810. *https://doi.org/10.1016/j.jcis.2021.08.134*

20 Jing X, Tian W, Linga R, Da B, Gerard M, Jean-Marie B, Lu Zh (2020) Hydrogen Energy Publications 45:7981-8001. *https://doi.org/10.1016/j.ijhydene.2020.01.052*

21 Torres D, Pinilla JL, Lazaro MJ, Moliner R, Suelves I (2014) Hydrogen Energy Publications 39:3698-3709. *https://doi.org/10.1016/j.ijhydene.2013.12.127*

22 Jing X, Da B, Jean M, Lu Zh (2021) J Clean Prod 320:879-884. *https://doi.org/10.1016/j.jclepro.2021.128879*

23 Henao W, Cazaña F, Tarifa P, Romeo E, Latorre N, Sebastian V, Delgado J, Monzón A (2020) Chem Eng J 20:103-126. *https://doi.org/10.1016/j.cej.2020.126103*

24 Bayat N, Meshkani F, Rezaei M (2016) Int J Hydrog Energ 30:13039–13049. *https://doi.org/10.1016/j.ijhydene.2016.05.230*

25 Osipov A, Sidorchik I, Shlypin D, Borisov V, Leontieva N, Lacrenov A (2021) Catalysis in Industry 13:244-251. *https://doi.org/10.1134/S2070050421030089*